

Bonded semiconductor interfaces with twist and tilt rotation: TEM analysis supported by molecular dynamics structure modelling

T. Wilhelm*, V. Kuhlmann, and K. Scheerschmidt

Max Planck Institute of Microstructure Physics, Weinberg 2, 06120 Halle, Germany

Received 17 September 2006, revised 26 March 2007, accepted 26 March 2007

Published online 11 July 2007

PACS 61.72.Ff, 61.72.Mm, 68.08.De, 68.37.Lp, 71.15.Pd

Regular dislocation networks have been created by hydrophobic wafer direct bonding of (001) oriented Si wafers. The dislocation densities depend on the (arbitrary) rotational misorientation of the wafers in [001] (twist) and the miscut (tilt). The interfaces have been studied by transmission electron microscopy. Additionally, molecular dynamics simulations have been used to study the system. The simulation of arbitrary angles and multiple misorientations prevents the use of periodic boundary conditions and necessitates the calculation of large cells with up to 500 000 atoms.

© 2007 WILEY-VCH Verlag GmbH & Co. KGaA, Weinheim

1 Introduction The controlled placement of biological molecules onto silicon surfaces is crucial for the design and implementation of new bioelectronics devices (biochips, biosensors etc.). Our approach to this challenge is to utilise the electrostatic forces between charged biomolecules and buried dislocation networks near Si surfaces to adsorb the biomolecules to the Si in a self-organised way [1].

Regular dislocation networks can be formed by wafer direct bonding of Si substrates [2] and of SOI substrates [3]. Generally, 2 different misorientations determine the type of network that forms: The miscut of the wafers (tilt misorientation), which are normally not ideally (001) oriented, leads to the formation of surface steps. Recently a method to accurately control the wafer orientation has been developed that avoids these steps [4]. The arbitrary rotation along [001] (twist misorientation) results in the formation of a regular screw dislocation network. Reactions of these dislocations lead to the formation of 60° dislocations [5] which can be seen as zigzag lines under suitable diffraction conditions in the TEM [6]. If the separation of the edge dislocations D_{tilt} is much larger than the spacing of the screw dislocations D_{twist} , then their interaction plays a minor role (Sample A, Fig. 1a), but for $D_{\text{tilt}} \approx D_{\text{twist}}$ the proportion of the 60° dislocation increases significantly (Sample B, Fig. 1b).

Molecular dynamics (MD) and image simulations have been used in the past to simulate dislocation networks with special twist angles which allow for periodic boundary conditions but without tilt misalignment [7]. In order to simulate the structure from Fig. 1b, including twist and tilt, several challenges have to be met:

The large dislocation distance suggests to calculate a large supercell. The boundary conditions are non-periodic which again requires the calculation of a bigger volume. Due to the presence of surface steps the cutting and placement of the simulated wafers at the start of the simulation is not trivial.

2 Experimental section The samples A and B were bonded under cleanroom conditions; for sample A, n-type material (~5–30 Ω cm) was used, for sample B p-type material (~15 Ω cm). After bonding,

* Corresponding author: e-mail: twilhelm@mpi-halle.mpg.de, Phone: +49(0)3455582975, Fax: +49(0)3455511223

sample A was annealed 2 h at 1000 °C in Ar, sample B was annealed 4 h at 1050 °C in O₂. The twist misorientation was 3.4° for sample A and 1.5° for sample B. For the plan-view TEM investigations, the samples were cut at an angle of 25° to the bonded interface. Further preparation included mechanical grinding, polishing, dimpling and Ar ion milling. The microscope used was a Phillips CM20T, operated at 200 kV.

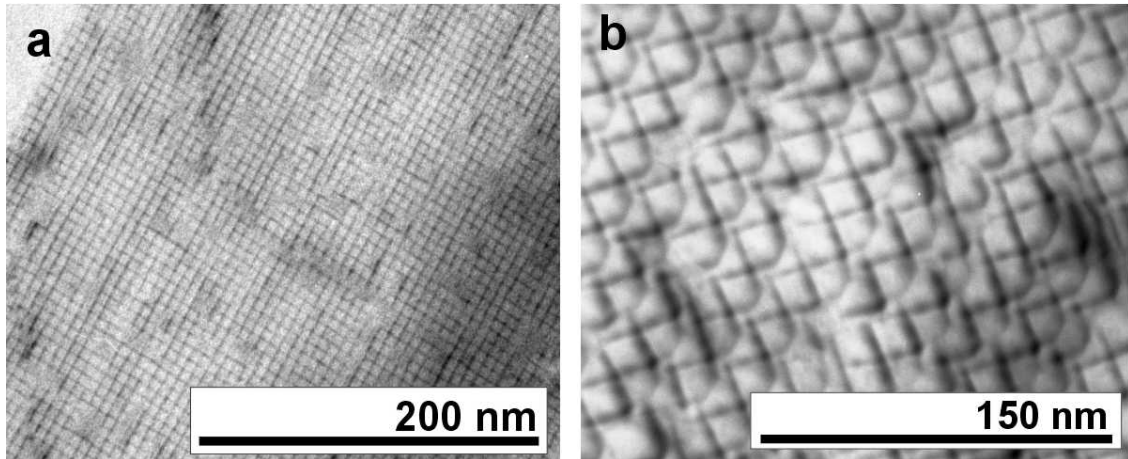


Fig. 1 TEM plan view images of dislocation networks; a) sample A, $D_{\text{tilt}} = 180$ nm, $D_{\text{twist}} = 6.5$ nm; b) sample B, $D_{\text{tilt}} = 24$ nm, $D_{\text{twist}} = 17$ nm.

3 Modelling Because of the large number of atoms involved in the relaxation of bonded interfaces only classical MD calculations will be used, which enable the atomistic structure simulations of nanoscopic systems as the one considered above. For given empirical atomic interaction potentials one has to integrate the Newtonian equations of atomic motion with time steps of the order of 0.5 fs to ensure the proper calculation of surface modes by embedding the model in a suitable surrounding [8].

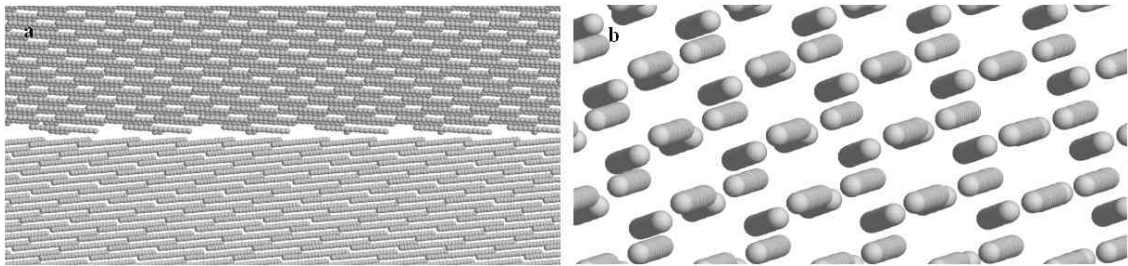


Fig. 2 Atomic model of sections of a $14 \times 10 \times 23$ nm³ cell containing 168291 Si atoms before the MD simulation; a) steps and holes exist at the interface; b) the [001] view shows the undisturbed columns of Si atoms in the two perfect crystals.

Figure 2 shows a typical start model for an interface to be bonded, Fig. 3 the energy behaviour of the system during the simulation and Fig. 4 snapshots after the MD-relaxation, with overviews approximately along the interface in Figs. 2a and 4a and the atomic rows across the (001) interface in Figs. 2b and 4b. To ensure structure relaxations with reordering processes at the interface, we apply MD-annealing cycles up to 900K with equilibration of the system at every temperature step, cf. Fig. 3.

To control the system temperature, either all particle velocities may be slightly rescaled at each time step, or solely the outer layers of the structure model. In the latter case, the energy dissipation and thus

the dynamic bonding behaviour may be controlled by the transfer rates of the kinetic energy at the borders of the model describing an energy flux into a macroscopic substrate.

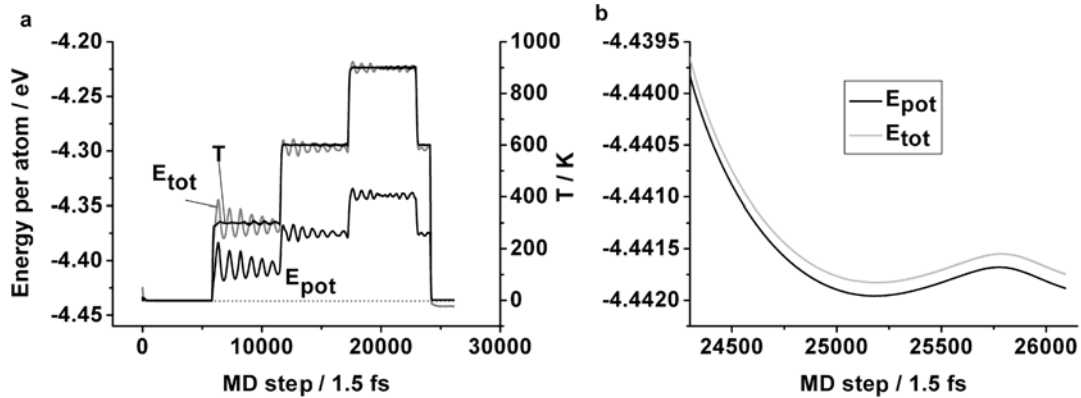


Fig. 3 Temperature T , total and potential energy E_{tot} , E_{pot} progression during the MD experiment; a) T and E for the whole simulation; b) the energies at the end of the experiment.

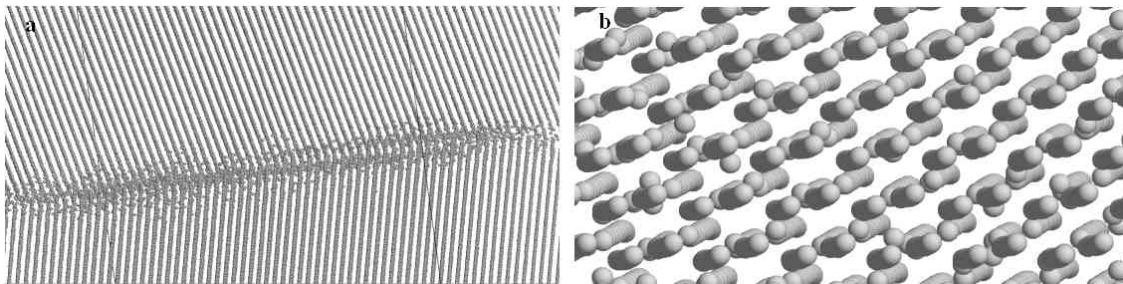


Fig. 4 Snapshots of the relaxed cell after the experiment; a) the now closed interface exhibits a visibly disturbed crystal structure; b) in the [001] view, a bending of the Si atom columns can be observed.

As empirical potentials we apply either well fitted Tersoff potentials, or, to enhance MD, an analytic bond order potential (BOP) based on the tight binding (TB) model, as it preserves the essential quantum mechanical nature of atomic bonding. The BOP achieves $O(N)$ scaling by diagonalising the orthogonal TB-Hamiltonian recursively and is recognised as a fast and accurate model for atomic interactions [9].

The molecular dynamics simulation of wafer bonding starting with two perfect and parallel-oriented Si blocks with perfectly aligned and reconstructed (001) surfaces yields perfectly bonded structures, bonding over steps introduce partial dislocation configurations [10]. A 90° twist boundary creates the special “dreidl”-interface configuration [11], whereas small twist-rotations yields more or less perfect screw dislocation networks [7].

The MD-relaxed models are the basis to calculate the TEM images. The structures are divided into thin slices so that for perfect structures only one atomic plane would be contained. Relaxed structures with bent and tilted atomic planes make this procedure difficult and create artefacts. The image simulations are carried out using the EMS package [12] for multi-slice simulations of the scattered wave, the diffraction contrast is then calculated by selecting relevant reflexes with suitable own scripts and applying the contrast transfer theory within the Digital Micrograph™ imaging software.

Figure 5 shows the diffraction pattern corresponding to the simulated wave in the Fourier space, and two dark field TEM images related to the selected reflexes. For comparison, Fig. 6 shows the equivalent TEM dark field images from the sample B (cf. Fig. 1b).

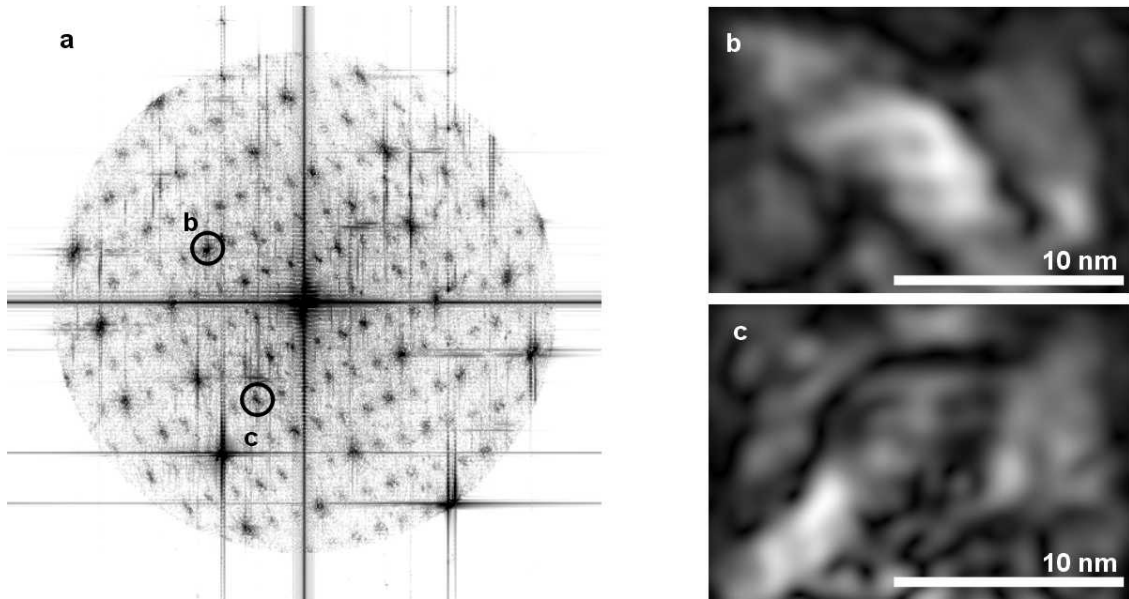


Fig. 5 Images calculated from a MD relaxed cell of $19 \times 14 \times 31 \text{ nm}^3$ containing 359968 Si atoms. a) Simulated diffraction pattern with many unwanted reflexes due to the small cell size and border effects; the $\{022\}$ reflexes used for the images (b) and (c) are marked. b, c) Simulated TEM dark field images using the reflexes marked in (a).

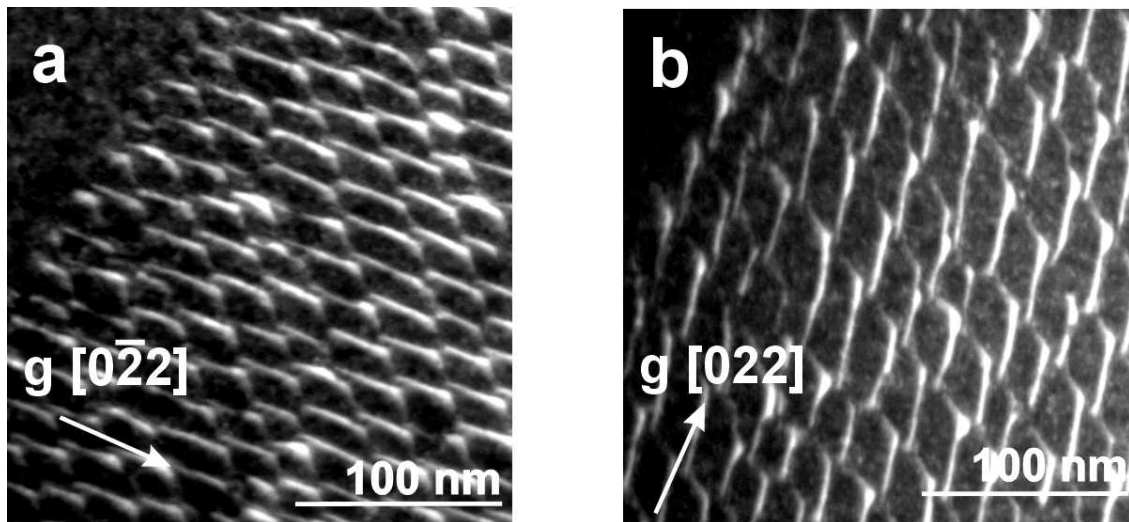


Fig. 6 Dark field TEM plan view images of sample B using two perpendicular $\{022\}$ reflexes.

The simultaneous consideration of both twist and tilt during the modelling of the interface bonding and the large dislocation distances for small misorientations suggest calculations with large supercells and the use of open boundaries. However, constant volume (NVE ensemble) calculations for models with open boundaries create unwanted surface relaxations and border effects.

Constant pressure calculations (NpT ensemble) or an elastic coupling to the bulk wafer would enable the relaxation of the cell dimensions and the application of an outer pressure. Periodic boundary conditions require the coincidence site lattice restrictions to be met via a proper selection Pythagorean triples. For small twist and tilt angles, this necessitates enormous numbers of atoms (several millions) to be

included in the supercells, and should be applied in future, detailed simulations. The present simulations are confined to non-periodic subunits, even though this leads to the generation of artefacts at the cell borders.

5 Conclusions Molecular dynamics calculations have been carried out to simulate a wafer bonding experiment with arbitrary twist and tilt misorientations, requiring the use of large supercells and non-periodic boundary conditions. While the calculations yield relaxed bicrystals with closed interfaces, the simulated TEM dark field images still contain many artefacts and are difficult to interpret. Future work will focus on larger supercells containing $>10^6$ atoms.

Acknowledgements The authors thank M. Reiche for providing the samples. The project SOBSI (self-organised pattern formation at silicon interfaces) is financially supported by the Volkswagenstiftung.

References

- [1] M. Kittler et al., *Mater. Sci. Eng. C* **26**, 902 (2006).
- [2] M. Reiche et al., *Inst. Phys. Conf. Ser.* **157**, 447 (1997).
- [3] C. Chen et al., *Philos. Mag. A* **80**, 881 (2000).
- [4] K. Rousseau et al., *Philos. Mag.* **85**, 2415 (2005).
- [5] T. Akatsu, R. Scholz, and U. Gösele, *J. Mater. Sci.* **39**, 3031 (2004).
- [6] A. Boussaid, M. Fnaiech, F. Fournel, and R. Bonnet, *Philos. Mag.* **85**, 1111 (2005).
- [7] K. Scheerschmidt and V. Kuhlmann, *Interface Sci.* **12**, 157 (2004).
- [8] K. Scheerschmidt, in: *Theory of Defects in Semiconductors*, edited by D.A. Drabold and S.K. Estreicher, *Topics in Applied Physics*, Vol. 104 (Springer, Heidelberg, 2006), p. 195.
- [9] A.P. Horsfield, A.M. Bratkovsky, M. Fearn, D.G. Pettifor, and M. Aoki, *Phys. Rev. B* **53**, 12694 (1996).
- [10] D. Conrad, K. Scheerschmidt, and U. Gösele, *Appl. Phys. A* **62**, 7 (1996).
- [11] A.Y. Belov, D. Conrad, K. Scheerschmidt, and U. Gösele, *Philos. Mag. A* **77**, 55 (1998).
- [12] P.A. Stadelmann, *Ultramicroscopy* **21**, 131 (1987).